A collimated flow driven by radiative pressure from the nucleus of quasar Q 1511+091[*]

R. Srianand[1], Patrick Petitjean[2,3], Cedric Ledoux[4] & Cyril Hazard[5]

[1] *IUCAA, Post Bag 4, Ganeshkhind, Pune 411 007, India - email: anand@iucaa.ernet.in*
[2] *Institut d'Astrophysique de Paris – CNRS, 98bis Boulevard Arago, F-75014 Paris, France - email: petitjean@iap.fr*
[3] *LERMA, Observatoire de Paris, 61 avenue de l'Observatoire, F-75014 - Paris, France*
[4] *European Southern Observatory, Alonso de Córdova 3107, Casilla 19001, Vitacura, Santiago, Chile- email: cledoux@eso.org*
[5] *Institute of Astronomy, Madingley Road, CB3OHA Cambridge, United Kingdom*

ABSTRACT
High velocity outflows from quasars are revealed by the absorption signatures they produce in the spectrum of the quasar. Clues on the nature and origin of these flows are important for our understanding of the dynamics of gas in the central regions of the Active Galactic Nucleus (AGNs) but also of the metal enrichment of the intergalactic space. Line radiation pressure has often been suggested to be an important process in driving these outflows, however no convincing evidence has been given so far. Here we report observation of a highly structured flow, toward Q 1511+091, where the velocity separations between distinct components are similar to O VI, N V and C IV doublet splittings with some of the profiles matching perfectly. This strongly favors the idea that the absorbing clumps originate at similar physical location and are driven by radiative acceleration due to resonance lines. The complex absorption can be understood if the flow is highly collimated so that the different optically thick clouds are aligned and cover the same region of the background source. One component shows saturated H I Lyman series lines together with absorptions from excited levels from C II and Si II but covers only 40% of the source of continuum. The fact that clouds cover only part of the small continuum source implies that the flow is located very close to it.

Key words: *Quasars:* absorption lines – *Quasars:* individual: Q 1511+091

1 INTRODUCTION

Comprehensive understanding of the nature and origin of gas flows in the very central regions of AGNs is elusive despite decades of intensive investigation. Presence of outflows with very large velocities ($\sim$20000 km s^{-1}) is revealed by the broad as well as narrow absorption lines (BALs and NALs) observed in the spectrum of AGNs. It has been suggested for long that the momentum transferred through resonance absorption lines could play an important role in driving these flows as it does in the case of O star winds (Castor, Abbott & Klein 1975; Arav, Li, & Begelman 1994). However, signatures of acceleration, though claimed to be noted in nearby Seyfert galaxy NGC 3515 (Hutchings et al. 2001), are not generic.

A possible way to reveal line-driven acceleration is the presence of absorption features with velocity separation similar to doublet and/or multiplet splittings (a consequence of the so-called "line-locking" effect). Such a structure in absorption is achieved when there is a reduction in the flux that drives the far away gas element due to line absorption produced by the gas closer to the QSO (Scargle 1973; Braun & Milgrom 1989). For higher efficiency, the gas from different elements of the flow must cover the same region of the background source. Since the gas producing intrinsic absorption is known to cover the background source only partially (Petitjean et al. 1994; Hamann 1997; Barlow & Sargent 1997), line-locking can be achieve in this case if the flow is somehow collimated. This may be one of the reasons why tentative evidences for line-locking (Foltz et al. 1987; Srianand 2000; Srianand & Petitjean 2001; Vilkoviskiji & Irwin 2001) as well as double trough (the so-called Lyman-alpha ghost) seen in the mean profile of BALs (Weymann et al. 1991; Korista et al. 1993; Arav, Li & Begelman 1994) are not completely
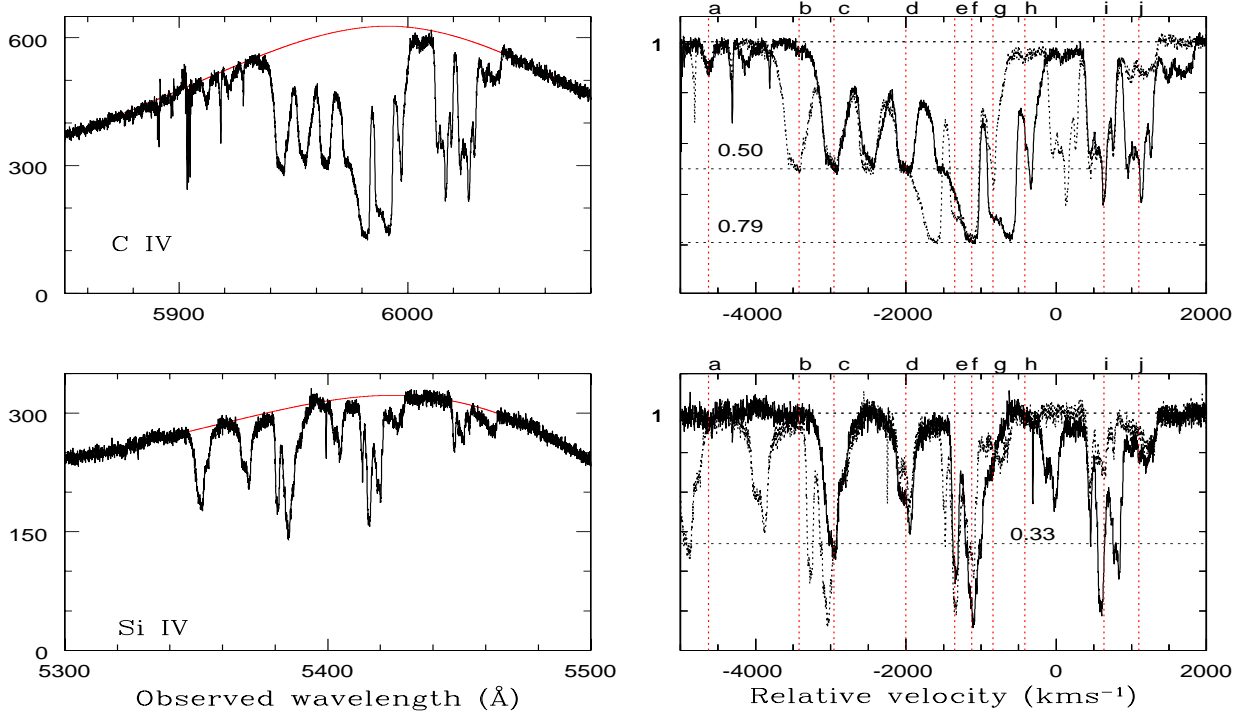
Figure 1. The left-hand side panels show the fit to the effective continuum (continuum plus broad emission line) of QSO spectrum in the C IV (top) and Si IV (bottom) emission line regions. Right-hand side panels show the corresponding normalised fluxes on a velocity scale with respect to $z = 2.878$. The y-axis in the left and right panels give the observed spectrum (without flux calibration) and normalised flux respectively. The continuous and dotted profiles are for the first (C IVλ1548 and Si IVλ1393) and second (C IVλ1550 and Si IVλ1402) members of the doublets respectively. The horizontal dashed lines in each panels give the residual flux expected for different covering factors (as indicated above each line). If the absorbing gas covers the continuum source only then the expected total covering factor of the background source is ~ 0.5 and ~ 0.70 for the C IV and Si IV lines respectively. These values are obtained using the relative flux ratios of emission lines and continuum at the position of the absorption line from low dispersion spectra of Sargent et al (1988).

convincing. In this paper we present clear evidence for a flow that is highly structured through radiative pressure modulated by absorption in different resonance lines.

2   OBSERVATIONS

We have used the Ultra-violet and Visible Echelle Spectrograph UVES (D'Odorico et al. 2000) mounted on the ESO KUEYEN 8.2 m telescope at the Paranal observatory on April 4-7 2000 to obtain a high-spectral resolution spectrum of the $z_{\rm em} = 2.878$ and $m_{\rm V} = 17$ quasar Q 1511+091. Two standard dichroic settings have been used to observe with both arms of the spectrograph at the same time. The final wavelength range is $3260-10,000$ Å. The slit width was 1 arcsec resulting in a resolution of $\sim$45000. The total exposure time was 10 hours in seeing conditions better than 0.8 arcsec full width at half maximum. The data were reduced using the UVES pipeline, a set of procedures implemented in a dedicated context of MIDAS, the ESO data reduction package. The main characteristics of the pipeline is to perform a precise inter-order background subtraction for science frames and master flat-fields, and to allow for an optimal extraction of the object signal rejecting cosmic ray impacts and performing sky-subtraction at the same time. The reduction is checked step by step. Wavelengths were

Table 1. Covering factor of the absorbing gas

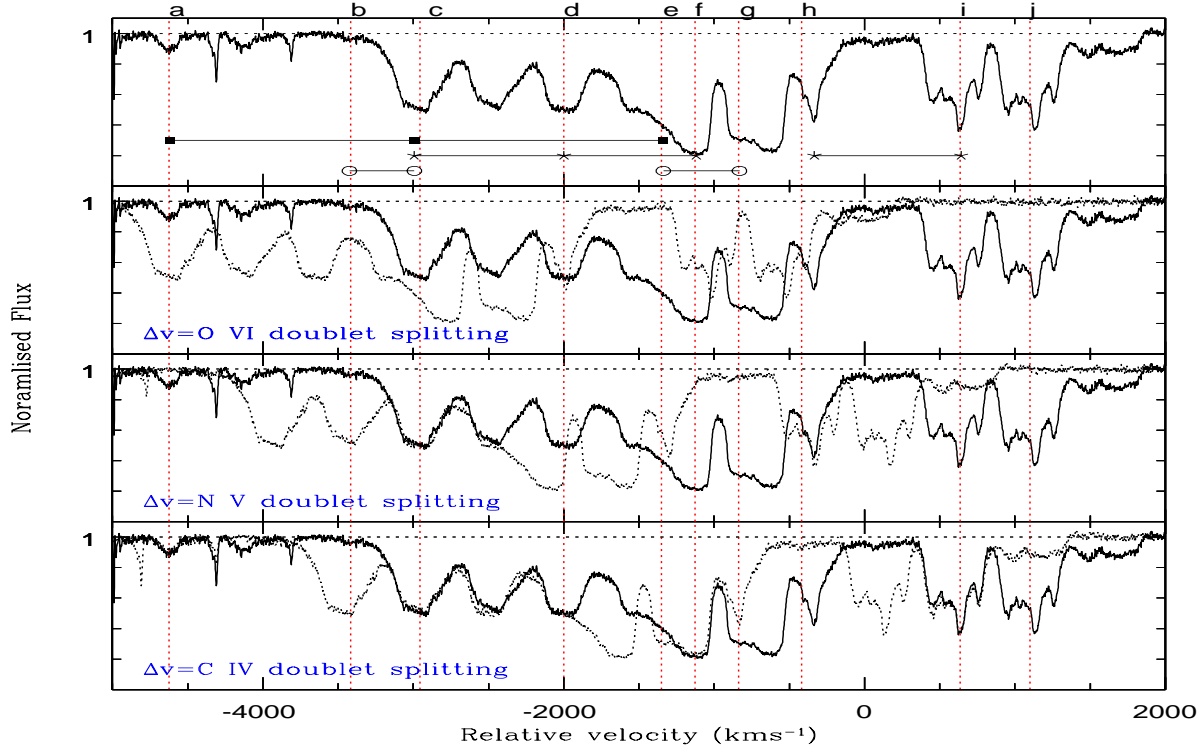| Component	$z_{\rm abs}$	species	$f_{\rm c}$
a	2.8186	C IV	0.10±0.04
c	2.8398	C IV	0.48±0.02
d	2.8523	Ly α^b	0.30±0.01
		Ly series	0.30−0.40
		C IV	0.50±0.01
		Si IV	0.30±0.05
		N V^b	0.46±0.01
e	2.8607	Ly α^a	$\leqslant 0.42$
		Ly series	0.40−0.45
		Al III	0.43±0.03
		C IV	$\leqslant 0.57$
		Si IV	$\leqslant 0.49$
f	2.8641	C IV	0.77±0.01
		N V	0.75±0.02
j(blue)	2.8908	Ly α	$\geqslant 0.15$
		C IV	$\geqslant 0.10$
		Si IV	0.28±0.12
		N V	0.22±0.03
j(red)	2.8934	Ly α	$\geqslant 0.15$
		C IV	$\geqslant 0.10$
		Si IV	0.17±0.07
		N V	0.18±0.02

^{b} Line saturation is assumed

Figure 2. C IV absorption profile (top panel and solid line in other panels). The same profile, but shifted by different velocity separations, is overplotted as a dotted line in the other panels (respectively O VI, N V and C IV from top to bottom). Different velocity components that are separated by C IV (circle), N V (star) and O VI (filled square) doublet splittings are marked in the top most panel. The vertical dotted lines mark the position of various distinct component identified in the flow.

corrected to vacuum-heliocentric values and individual 1D spectra were combined together. This resulted in a S/N ratio per pixel of 25 at $\sim$3600 Å and 80 at $\sim$6000 Å. Typical errors in the wavelength calibration are less than ~ 0.5 km s^{-1}.

3 COVERING FACTOR

The UVES spectrum of Q 1511+091 over the C IV and Si IV emission line wavelength ranges is shown in the left-hand side panels of Fig. 1 together with the fit to the effective continuum (i.e., quasar continuum plus broad emission lines) we used to normalize the spectrum. Partial coverage of the absorbing gas implies some residual at the bottom of absorption lines even if they are heavily saturated. Partial coverage is apparent when the two resolved lines of a doublet, with different oscillator strengths, have the same apparent residuals without going to zero. This is obviously the case for most of the components in the C IV flow toward Q 1511+091. The two absorption lines of the C IV doublet corresponding to components **a**, **c**, **d** and **f** have exactly the same apparent depths over their profiles. It can be seen on right panels of Fig. 1 that when the spectrum is shifted by the velocity separation of the two lines of the C IV doublet, the profiles coincide nearly perfectly for most of the wavelength range. Using the method described in Srianand & Shankaranarayanan (1999) we estimated the covering factor for different species in individual components. The results are given in Table. 1.

It is possible to say that different part of the flow cover the

same background region. Indeed, it can be noted that when C IVλ1550 of one component, say component 1, overlaps with C IVλ1548 of another component, say component 2, the resultant optical depth, although smaller than 0.5 is not the sum of the optical depths of the two absorption lines. This is particularly striking for C IVλ1548 of component **e** and C IVλ1550 of component **d** or for C IVλ1548 of component **g** and C IVλ1550 of component **e**. This can be understood if one of the saturated components, say component 1, is shielding the other component, say component 2 in such a way that the flux supposed to reach component 2 in C IVλ1548 is absorbed completely by component 1 in C IVλ1550. This explains why, although blending is apparent, the C IVλ1548 profile matches so closely the same profile shifted by the velocity splitting between the two C IV lines (see Fig. 2). This shows that at least part of the flow is collimated and covers the same part of the emitting region.

4 SIGNATURES OF LINE-DRIVEN ACCELERATION

The most striking observation in this flow is that the velocity differences between distinct components coincide with various doublet velocity splittings (see Fig 2 and Table. 2). The most apparent coincidences are seen for the N V doublet splitting. Both the C IV lines of components **c** and **d** match very closely. Not only the velocity difference between the centroids of the two components is very close to the

Table 2. Velocity splitting among distinct components

Doublet	splitting (km s^{-1})	components	separation (km s^{-1})
C IV	499	**b - c**	495
		e - g	499
N V	962	**c - d**	969
		d - f	930
		e - h	924
O VI	1650	**a - c**	1660
		c - e	1625

N V doublet splitting but also the residual intensities and the widths of the components ($FWHM \sim 300$ km s^{-1}) are nearly identical. Very good matchings are also seen for one of the lines of **e** and **h** and **d** and **f**. In addition to this we notice that components **h** (defined by weak albeit broad C IVλ1550 and O VI absorptions) and **j** are separated by the N V doublet splitting (see Fig. 2). For the O VI splitting, coincidences are seen for components **a** and **c**, **c** and **e** (with similar residuals). This is complemented by coincidences with C IV splitting between **b** and **c** but mostly between **e** and **g** and between component **i** and diffuse absorption component **j**.

In a spectral range where crowding of absorption lines is so important, chance coincidences are possible. In order to consider the probability that such coincidences occur by chance, we randomly populated the observed velocity range with 10 components. Using 10^6 realizations we find a probability of 6×10^{-4} for the occurrence of, at least two coincidences, each with the velocity splittings of the O VI , N V or C IV doublets with a matching uncertainty of ±20 km s^{-1}. If we introduce the additional condition that at least two coincidences occur between three components in O VI splitting (like the one seen among **a-c** and **c-e**) the probability becomes $< 10^{-6}$ for a wavelength matching uncertainty of ±20 km s^{-1}.

This low probability for mere velocity coincidence together with tight matching of some of the profiles and consistent covering factors clearly confirms the line-locking situation in this system. It must be noted that, although the corresponding wavelength range is crowded by intervening lines, additional coincidences are apparent between the corresponding O VI absorptions. In addition, the velocity separation between components **a** and the red component of **i** ($\Delta_v = 5830$ km s^{-1}) is very close to the N V to Lyα velocity splitting. Therefore, all components are connected by a complex set of coincidences. Under the assumption that line-locking is structuring the flow, it is expected that components with larger covering factors be located closer to the source. This would imply in that case that the flow is an accelerating wind.

5   DISCUSSION

The physical conditions in part of the flow can be investigated from the very peculiar component **e** at $z_{abs} = 2.8606$ (-1350 km s^{-1} in Fig. 2). Absorption lines from H I Lyman series lines as well as excited levels of singly ionized species C II and Si II are present (see Fig. 3 and from C II to P V. However, none of the Lyman series absorption lines
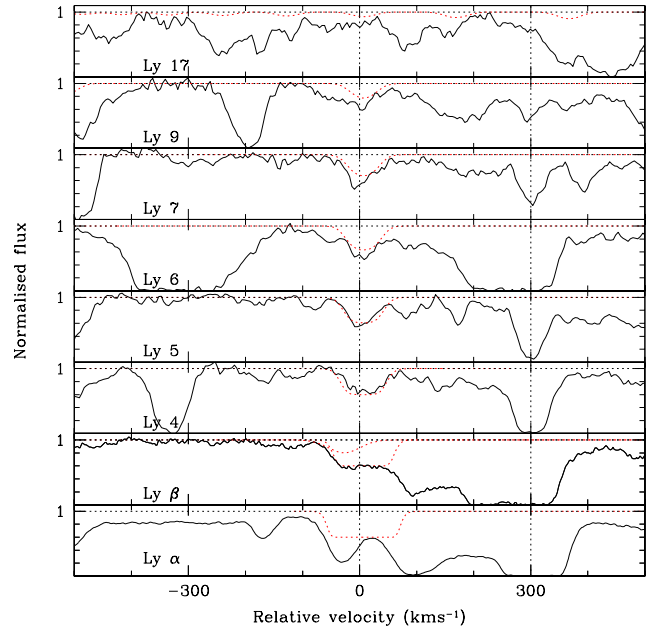

Figure 3. Velocity plot of Lyman series absorption lines produced by component **e** at $z_{abs} = 2.8606$ toward Q 1511+091. The best fitted profile (dotted line) is obtained considering the gas covers only 40% of the continuum emission (from the accretion disk). Note that a weak additional intervening Lyman α line is blended with the Lyman β line. The effect of partial coverage can be appreciated by comparing the profiles of this component with that of an intergalactic absorption with similar amount of H I seen at 300 km s^{-1}.

are dark. Lyman-α is not even seen as a distinct component when it should be conspicuous. Similar situation was observed by Telfer et al. (1998) toward QSO SBS 1542+531. From the flat bottom of the Lyman-β line, it is apparent that the cloud does not cover the background source completely. Higher Lyman series lines are well fitted with a covering factor of the order of 0.4. It must be noted that the emission lines for the corresponding transitions are negligible compared to the continuum. In addition, such a low covering factor can not be accommodated by scattered light (Ogle et al. 1999) . Therefore, it can be concluded that *the cloud covers only about 40% of the central source of continuum* whose radius is of the order of 10^{-3} pc. All neutral hydrogen lines can be fitted consistently (see Fig. 3) with $f_c = 0.4$ and $\log N(\text{H I}) \sim 16.30$. A consistent model for all other absorption lines is found with this covering factor (see Fig. 4) and using the Al III and Si III profiles as templates for, respectively, the singly-ionized and high-ionization species. The difference between the two profiles is mainly due to an extra component in the red wing that is seen in Si III and other higher ionization lines. Note that although the centroids of the lines are the same, the width of the lines increases with ionization.

It is striking to note that with this covering factor, the ratios C II*/C II and Si II*/Si II are found to be both of the order of two which is the value expected in case of thermal equilibrium. Given the ionization state of the gas (see below), the temperature is most probably larger than 10^4 K, and from
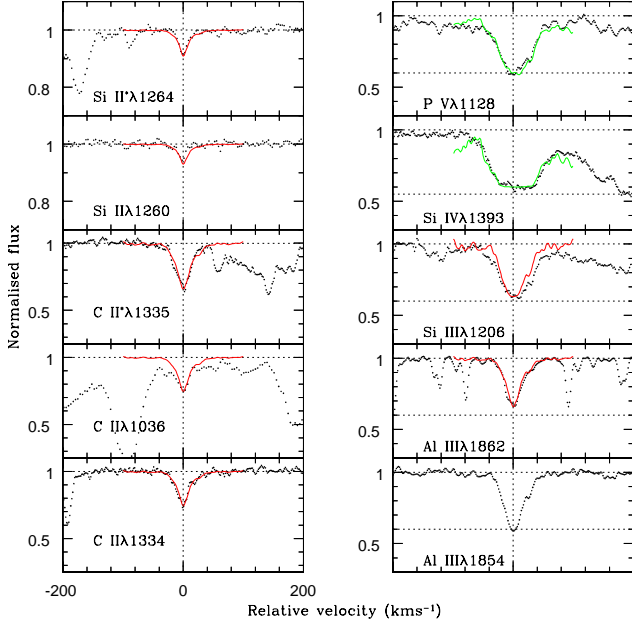
Figure 4. Fits of the absorption profiles in component **e** at z_{abs} = 2.8606 toward Q 1511+091. The observed profile of Al IIIλ1854 is used as a template to fit the singly ionized species. The profile are fitted assuming a covering factor of 0.4 and by varying the central optical depth preserving the profile function given by the template. P V and Si IV profiles are fitted using the Si III profile as the reference template. The difference between the two profiles is mainly due to an extra component in the red wing that is seen in Si III and other higher ionization lines.

the thermal equilibrium between populations of Si II levels we can derive the electronic density $n_e \geqslant 1.3 \times 10^3 \ T_4^{0.5}$ cm^{-3} (T_4 is the temperature in the units of 10^4 K). For a Mathews & Ferland (1987) QSO ionizing spectrum, and using the constraints from observed ion ratios, the ratio of the ionizing photon density to the hydrogen particle density (the so-called ionization parameter, U) can be shown to be in the range $-2.0 < \log U < -0.6$. The metallicities are most probably larger than solar. This is somewhat consistent with the typical values obtained for the Broad Line Region, $-1.0 < \log U < -0.0$ and $10^9 \leqslant n_e \leqslant 10^{11}$ cm^{-3}, although the density is probably smaller in the cloud (see below). Assuming a typical luminosity density at the Lyman limit of 10^{31} erg s^{-1} Hz^{-1}, and a spectral index of -1.6 the maximum distance of the absorbing gas from the source is $15.75\sqrt{1/nU}$ kpc. The lower limit on n_e derived above suggests the gas has to be at a distance less than a few kpc from the ionizing source.

From the absence of absorption due to C III$^*\lambda$1176 originating from an excited metastable level, we derive an upper limit on the density of 8×10^9 cm^{-3}. This gives a minimum distance of a few 10^{-1} pc. Thus the observations are consistent with the absorbing gas being inside or close to the BLR. For a spherical absorbing cloud the particle density is $\sim N(\text{H})/\sqrt{f_c}R_c$, where R_c and $N(\text{H})$ are the radius of the continuum emitting region and the total hydrogen column density of the absorbing gas (in the range, $10^{19} \leqslant$

$N(\text{H}) \leqslant 10^{20}$ cm^{-2}, from the models) respectively. For the lower limit on density we get, $R_c \leqslant 0.04 \ T_4^{-0.5}$pc.

The largest blue-shift observed in the C IV profile is much smaller than the typical terminal velocities of BAL flows. This probably means that the gas could be further accelerated. Indeed, for physical conditions similar to those observed in different components of the Q 1511+091 outflow, the line-radiation force is much larger than gravity even in the close proximity of the black-hole (de Kool & Begelman 1995) . Most of the hydrodynamical radiatively driven wind models predict the gas to reach terminal velocity at a distance of a few pc from the ionizing source (Arav et al. 1994). Lack of acceleration in components with velocity much lower than the terminal velocity could be accounted for if either our line of sight probes a small portion of a non-radial flow (Arav 1996) or the extra drag forces are at play in reducing the effective acceleration of the gas. In the case of Q 1511+091, the absorption lines are seen at redshift very close to or slightly higher than the systemic redshift. In addition, nearly perfect velocity matching with doublet splittings suggests that the direction of the flow is very close to our line of sight.

Disk winds have been suggested as the natural origin for ejected material from quasars giving rise to BAL systems (de Kool & Begelman 1995; Murray et al. 1995; Proga et al. 2000). In these models, a cylindrically symmetric disk wind is ejected away from the surface of the disk and is radiatively accelerated radially once exposed to the strong continuum source. Line-driven instabilities could lead to the formation of distinct velocity components seen in the flow (Feldmeier et al. 1997). Our observations illustrated in Fig. 5 support the basic mechanism at work in these models. It would be very interesting to constrain the acceleration over a large time-scale for our understanding of the nature of drag forces and in general the nature of the flow.

REFERENCES

Arav N., 1996, ApJ, 465, 617
Arav N. & Begelman M., 1994, ApJ, 434, 479
Arav N., Li Z., Begelman M., 1994, ApJ, 432, 62
Barlow T. A. & Sargent W. L. W., 1997, AJ, 113, 136
Braun E. & Milgrom M., 1989, ApJ, 342, 100
Castor J. I., Abbott D. C., Klein R. I., 1975, ApJ, 195, 157.
de Kool M. & Begelman M. C, 1995, ApJ, 455, 448
D'Odorico S., et al., 2000, SPIE, 4005,1
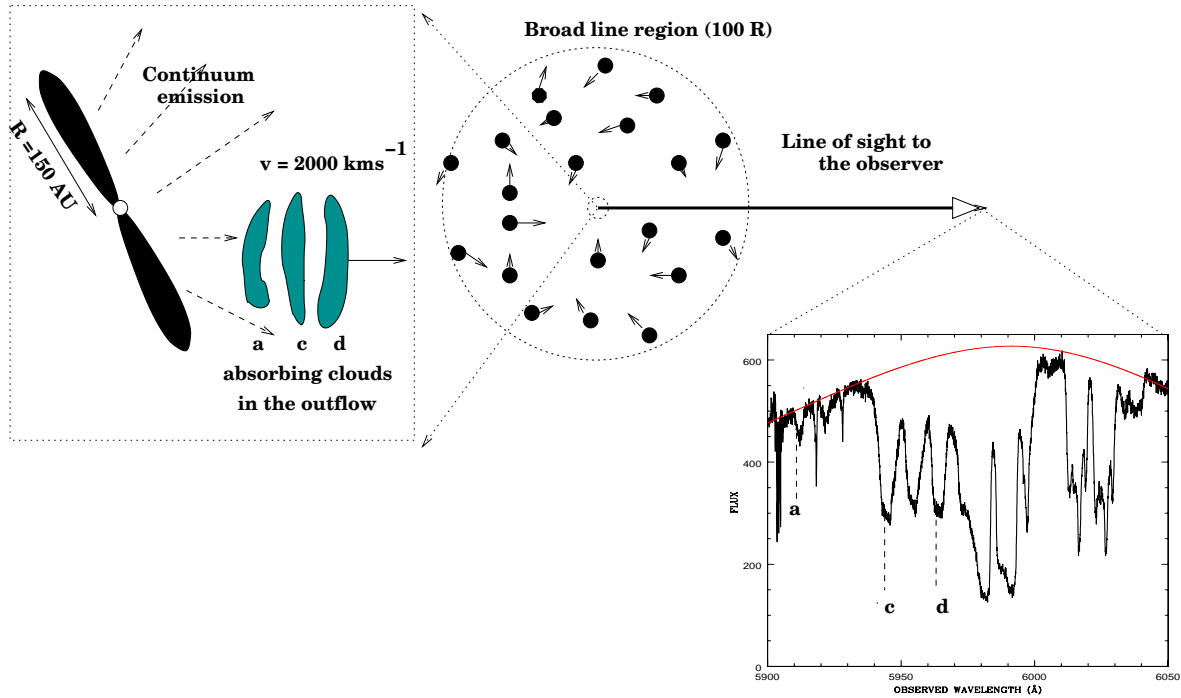Feldmeier A., Norman C., Pauldrach A., Owocki S., Puls J.,

Figure 5. Qualitative sketch of the relative position of the absorbing gas compared to the flux emitting region. The fact that some of the components of the outflow from Q 1511+091 cover only part of the source of continuum suggests that the absorbing gas is close to the continuum emission region. Typically the continuum is believed to originate from a region of size $R \sim 150$ AU. Reverberation mapping studies of AGNs indicate that the broad emission lines are produced by a region of radius at least 100 times that of the continuum emitting region. Thus it is most likely that at least part of the observed flow originate close to the inner boundary of the broad emission line region.

Kaper, L., 1997, in Mass ejection from Active Galactic Nuclei, ASP Conference Series, Vol, 128, p258.

Foltz C. B., Weymann R. J., Morris S. L., Turnshek D. A., 1987, ApJ, 317, 450

Hamann F., 1997, ApJS, 109, 279

Hutchings J. B., et al., 2001, ApJ, 559, 173

Korista T. K., Voit G. M., Morris S. L., Weymann R. J., 1993, ApJS, 88, 357

Mathews W. G. & Ferland G. J., 1987, ApJ, 323,456

Murray N., Chiang J., Grossman A., Voit M., 1995, ApJ. 441, 498

Ogle P. M., Cohen M. H., Mill J. S., Tran H. D., Goodrich R. W., Martel A. R., 1999, ApJS, 125, 1

Petitjean P., Rauch M., Carswell R. F., 1994, A&A, 291,29

Proga D., Stone J. M., Kallman T. R., 2000, ApJ, 543, 686

Sargent, W. L. W., Steidel, C. C., & Boksenberg, A. 1988, ApJS, 68, 539

Scargle J. D., 1973, ApJ, 179, 705

Srianand R., 2000, ApJ, 528, 617

Srianand R. & Petitjean P., 2001, A&A, 357, 414

Srianand R. & Shankaranarayanan, 1999, ApJ, 518, 672

Telfer R. C., Kriss G. A., Zheng W., Davidsen A. F., Green R. F., 1998, ApJ, 509, 132

Vilkoviskiji E. Y. & Irwin M. J., 2001, MNRAS, 321, 4

Weymann R. J., Morris S. L., Foltz C. B., Hewett P. C., 1991, ApJ, 373, 25